ARCHIVES OF ELECTRICAL ENGINEERING VOL. 61(1), pp. 57-67 (2012)

DOI 10.2478/v10171-012-0005-3

Field synthesis for the optimal treatment planning in Magnetic Fluid Hyperthermia

PAOLO DI BARBA[1], FABRIZIO DUGHIERO[2], ELISABETTA SIENI[2]

[1]*Department of Electrical Engineering, University of Pavia*
via Ferrata, 1-27100 Pavia, Italy

[2]*University of Padova, Department of Industrial Engineering*
via Gradenigo 6/a-35131 Padova, Italy

e-mail: paolo.dibarba@unipv.it, {fabrizio.dughiero,elisabetta.sieni}@unipd.it

(Received: 26.12.2011, revised: 11.01.2012)

Abstract: An automated procedure based on evolutionary computation and Finite Element Analysis (FEA) is proposed to synthesize the optimal distribution of nanoparticles (NPs) in multi-site injection for a Magnetic Fluid Hyperthermia (MFH) therapy. Evolution Strategy and Non dominated Sorting Genetic Algorithm (NSGA) are used as optimization procedures coupled with a Finite Element computation tool.

Key words: evolutionary algorithms, finite element analysis, magnetic fluid hyperthermia, optimal synthesis, coupled fields

1. Introduction

MFH uses magnetic nanoparticles (NPs) excited by a time-varying magnetic field to induce heat on the target volume in order to destroy the cancer tissues [1]. For the aim of the therapy magnetic NPs are suspended in a magnetic fluid, in order to facilitate their injection in the tumor region [2]. Then, the resulting NPs distribution depends on the position of local injections.

The first kind for MFH devices, that exhibits a large iron core, is installed at the Charité university hospital in Berlin [3]. In [4] a new design of the magnetic field source is proposed: the field is generated by means of an arrangement of coreless coils that was inspired by Loney solenoid system [4, 5]. The proposed design of the coils, with respect to existing devices, allows the modification of winding geometry and supplied currents according to patient size and region to be treated.

The uniformity of magnetic field is considered to be a prerequisite in order to have a uniform thermal field in the target tissues. In [4] the optimal shape design of the current carrying coils was proposed and solved, in order to obtain a uniform distribution of the magnetic field in the target tissue. Nevertheless, given the magnetic field on the target region, the region

temperature is related to NPs concentration that depends on the position of local injection of the magnetic fluid. Then, the main objective function is now the uniformity of the temperature distribution, to be maximized in the controlled region, and the target value of temperature (*e.g.*, 42°C for mild hyperthermia [6] or >60°C for thermal ablation [7]).

For this purpose, since in clinical hyperthermia based on magnetic fluids, the tumor region temperature depends also on concentration and distribution of NPs [8, 9], the coupled magnetic and thermal problem is solved considering a realistic NPs distribution [10]; the point is that, even if the magnetic field is maximally uniform in the treatment region, the thermal field might not have the same uniformity degree due to the non uniform-distribution of NPs in the tissues. In [11] a thermal problem was solved considering a non uniform distribution of the NPs power density evaluated experimentally [11, 12]. The relevant power density was used in [12] to optimize the position of NPs injections, in order to fulfill some therapeutically important constraints on the tumor temperature. However, in [12] the distribution of magnetic field was disregarded. Moreover, a gradient-based, local-search oriented algorithm was used for optimization.

In this paper, an automated procedure of optimization, based on evolutionary computing and FEA [13-15], is proposed in order to find the position of multiple NPs injections determining a tumor temperature close to the therapeutic value. A realistic NPs distribution [2] is considered to compute the power density, while the direct problem models both magnetic and thermal fields.

2. Mathematical model

In MFH therapy heat is generated by means of a time-varying magnetic field H that produces the rotation of nanoparticles and their magnetic moments in a biological fluid [2, 9]. In order to compute the temperature as a function of time and space in the treated region, a thermal transient problem coupled with a time-harmonics magnetic problem is solved. In the magnetic problem Maxwell equations are solved subject to appropriate boundary conditions [16], whereas in the thermal problem the Fourier equation [17], taking into account the blood perfusion [18], is solved.

2.1. Magnetic problem

The magnetic field source is a current-carrying winding composed of four concentric coils, J_m and J_c, as in Figure 1(a) [4, 10]. The target region Ω_T, i.e. the tumor, which must be appropriately heated, exhibits an elongated shape like that in Figure 1(b); in fact, the tumor shape generally has a similar form. The surrounding volumes, i.e. Ω_L and Ω_B, are target and control regions, respectively, where the temperature must be limited in order not to damage healthy tissues. In particular, the Ω_T region models healthy tissue around Ω_L; reference is made to a liver tumor in the abdominal cavity.

In the conductive regions Ω_T, Ω_L, and Ω_B the electromagnetic problem is solved in terms of the phasor $\dot{\overline{H}}$ of the magnetic field by means of the phasors of electric vector potential, $\dot{\overline{T}}$, and total magnetic scalar potential, $\dot{\Phi}$, respectively [18-19]:

$$\dot{\overline{H}} = \dot{\overline{T}} - \overline{\nabla}\dot{\Phi}, \tag{1}$$

where electric vector potential, $\dot{\overline{T}}$, and total magnetic scalar potential, $\dot{\Phi}$, fulfil the following equations:

$$\overline{\nabla}^2 \dot{\overline{T}} - j\omega\mu_0\sigma\dot{\overline{T}} = 0, \tag{2}$$

and

$$\dot{\Phi} = -\frac{j}{\omega\mu_0\sigma}\overline{\nabla}\cdot\dot{\overline{T}} \tag{3}$$

with μ_0 and σ magnetic permeability and conductivity of the medium, respectively, and ω is the field pulsation. In the air region, around conductive volumes, the magnetic field is derived by means of the reduced scalar potential, $\dot{\phi}_R$ [19]:

$$\dot{\overline{H}} = \dot{\overline{H}}_s - \nabla\dot{\phi}_R \ , \tag{4}$$

where the phasor of the reduced scalar potential, $\dot{\phi}_R$, fulfils the Poisson equation [15]:

$$\overline{\nabla}\cdot\mu_0\overline{\nabla}\dot{\phi}_R = \overline{\nabla}\cdot\mu\dot{\overline{H}}_s \, . \tag{5}$$

In turn, H_s is computed by means of the Biot-Savart formula:

$$\dot{\overline{H}}_s = \frac{1}{4\pi}\int_\Omega \dot{\overline{J}}_s \times \overline{\nabla}\left(\frac{1}{r_a}\right) d\Omega, \tag{6}$$

where r_a is the distance between source and field point, J_s is the driving current density (i.e. J_m or J_c) and Ω is the actual conductor element. At infinity, the reduced scalar potential is imposed to be vanishing.

After the solution of (1) in the conductive regions, Ω_T and Ω_B, the magnetic field phasor $\dot{\overline{H}}$ is used in the equation that models the power density generated [2], in the case of not-uniformly distributed NPs.

2.2. Thermal problem

The numerical solution of the direct problem is based on a FEA tool [11-12, 20] for three-dimensional transient thermal analysis. The governing equation is the Fourier one equipped with the blood perfusion term [8, 21]:

$$c_p\gamma\frac{\partial T}{\partial t} = \lambda\nabla^2 T - c_b w_b\left(T - T_a\right) + P \tag{7}$$

in a time interval of 300 s. In (7) λ is the thermal conductivity, c_p the specific heat, γ the density of the tissue and T the temperature. Moreover, T_a is the basal body temperature (at 37°C), w_b is the mass flow rate which depends on tissue and temperature, c_b is the blood specific heat [21].

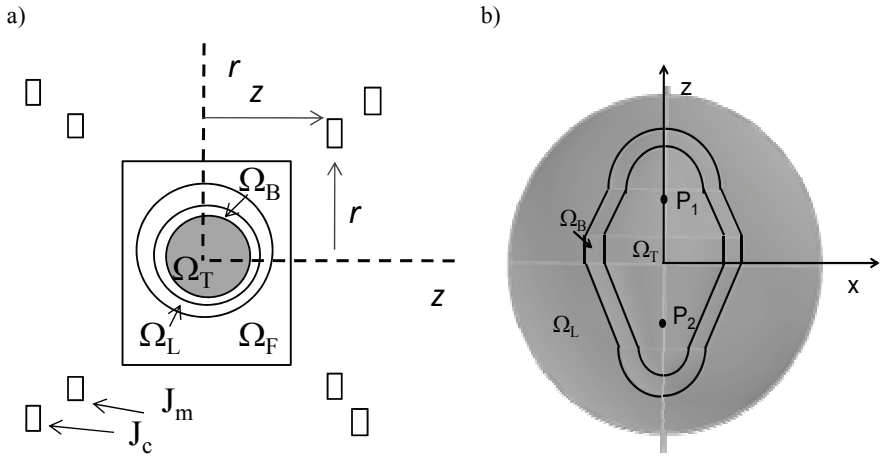

Fig. 1. Geometry of (a) MFH winding and (b) shape of the target volume Ω_T.

Given the magnetic field H obtained after solving the magnetic problem, the power density source, P, due to the NPs concentration, ϕ, is computed as follows [2]:

$$P(x,y,z,T,H,\phi) = \mu_o \pi \chi''(x,y,z,T,H,\phi) f H^2(x,y,z) \tag{8}$$

with f frequency of the magnetic field and χ'' imaginary part of the magnetic susceptivity, that in turn depends on the magnetic field H and the local concentration of NPs, ϕ:

$$\chi'' = \phi(x,y,z,\sigma) f_1(T) f_2(\xi(H,T)) f_3(\omega,\tau). \tag{9}$$

In (9), σ is the standard deviation that describes the NPs dispersion from the injection center. In particular, function f_2 depends on the Langevin parameter, ξ, which in turn depends on field intensity, H, and temperature, T; function f_3 depends on field pulsation, ω, and NPs relaxation time, τ [1], while function f_1 depends on temperature only. Let a spatial function of the NPs concentration, ϕ, with a Gaussian shape be assumed. For an injection point j it is:

$$\phi_j(x,y,z,\sigma) = \phi_0 e^{-\frac{1}{2}\left(\frac{(x-\eta_{j,x})^2}{\sigma^2} + \frac{(y-\eta_{j,y})^2}{\sigma^2} + \frac{(z-\eta_{j,z})^2}{\sigma^2}\right)} \tag{10}$$

with ϕ_0 constant concentration and $\eta_{j,i}$, $i = x, y, z$, Cartesian coordinates of the injection point. Equation (10) is written under the assumption that the diffusion speed is equal for the three orthogonal directions and uncorrelated with the one along the other directions. If multiple

injection points, N, are considered, the concentration ϕ of NPs in a volume is nothing but the superposition of N Gaussian functions:

$$\phi(x, y, z, \sigma) = \sum_{i=1}^{N} \phi_i(x, y, z, \sigma). \tag{11}$$

3. Synthesis problem

Given a magnetic field distribution in the tumor area, the aim of the synthesis problem is twofold: identify the optimal position of a few NPs injections in order to have a uniform distribution of the temperature field, taking into account the distribution of the magnetic NPs in the tumor, on one hand, and limit the diffusion of the NPs in the healthy tissue, on the other hand.

To solve the synthesis problem, a bi-objective optimization problem is formulated; the optimal placement of two NPs distributions with the same initial concentration is considered as the basic case. To this end, six design variables are defined: the positions of two NPs injections (x, y and z coordinates), and the dispersion, σ, i.e. the standard deviation of a Gaussian function used to describe the NPs distribution in the tissue.

In fact, the problem of heating the tumor region in a selective way can be cast as a multi-objective problem: the target temperature in the treating area must be over the therapeutic value in all points; however, in a mild hyperthermia treatment the temperature must not overcome a predefined value (e.g. 50°C as a safety threshold) in order not to damage healthy tissues. In the case considered, two objective functions have been defined.

3.1. Objective functions

The goal is to heat locally the tumor region as uniformly as possible: given the power density source as in (8), and the NPs distribution as in (11), the two objective functions characterizing the optimization problem are:

a) the volume of the tumor region in which the temperature is higher than a given threshold (*e.g.* 42°C), to be maximized [22], and
b) the sub-volume in which the temperature is higher than 50°C, to be minimized.

To evaluate the objective functions, the aforementioned volumes are recovered after uniformly sampling the region in the FE model. In particular, in the Ω_T region the first objective function is evaluated as follows:

$$R_1(T) = 100 \cdot \frac{N_T(T > 42)}{N_{T,tot}}, \tag{12}$$

where N_T is the number of temperature samples in the tumor region Ω_T for which the temperature is higher than 42°C, whereas $N_{T,\,tot}$ is the number of temperature samples in the whole tumor region, Ω_T. In turn, the second objective function is evaluated in the same volume region in the following way:

$$R_2(T) = 100 \cdot \frac{N_T(T > 50)}{N_{T,\,tot}}. \tag{13}$$

Therefore, the goal is to maximize (12) and minimize (13) with respect to the injection point coordinates and dispersion of the Gaussian distribution of NPs. The most general solution is given by the relevant Pareto front [12].

The magnetic problem is solved first in order to compute the magnetic field intensity in the whole domain. The input of the transient thermal problem is the power source (8) evaluated from the magnetic field intensity and the distribution of NPs (11). Then, (12) and (13) are evaluated from the thermal solution at t = 360 s.

In practice, two optimization strategies have been used in a comparative way, namely: single-objective Evolution Strategy and multi-objective Non-Dominated Sorting Genetic Algorithm, in order to find the best trade-off solutions of the problem.

3.2. Genetic algorithms

Despite the high number of function calls required, evolutionary and genetic algorithms have been successfully applied because they are gradient-free and therefore global-minimum oriented. They are based on the process of evolution, reproduction and selection of a population observed in nature. By means of mutation ad crossover operators, a set of parents generates a set of offsprings having characteristics inherited from the parents. Evolutionary computing found application in several branches of electromagnetics, like e.g. the optimal design of electrical machines [24]. ESTRA and NSGA are two major algorithms.

3.3. ESTRA: Evolution Strategy algorithm

In the class of evolutionary algorithms, the Evolution Strategy of the zero order (ESTRA) is an algorithm of single-objective optimization in which a parent, m, generate an offspring x, by means of a mutation operator [12].

3.4. NSGA: Non dominated Sorting Genetic Algorithm

The algorithm is able to approximate the whole Pareto front of a given multi-objective problem. The idea behind NSGA is that a selection method is used to emphasize current non-dominated solutions, and a niching method is used to maintain diversity in the population. NSGA varies from a simple GA in the way the selection operator is used. Crossover and mutation operators, in fact, remain as usual. However, before selection is performed, the population is ranked on the basis of the non-dominance level of an individual, and then a fitness value is assigned to each individual.

4. Results and discussion

A few optimal solutions have been obtained either maximizing the R_1 function [12], or – alternatively – minimizing the R_2 function [13]: both single-objective (SO) procedures started

from the same initial point using an Evolution Strategy (ESTRA) algorithm [12, 22] and two different solutions are found. The assumption of conflicting objectives seems to be assessed, because the two ($P_1(x_1, y_1, z_1)$, $P_2(x_2, y_2, z_2)$) pairs found are different as reported in Table 1. In Figure 2, an approximation of the 2D objective space is obtained after the SO optimizations; the R_2 values are represented as a function of (100-R_1) ones. The filled symbols represent the optimal solution found using ESTRA algorithm. Seemingly, a Pareto front is detected.

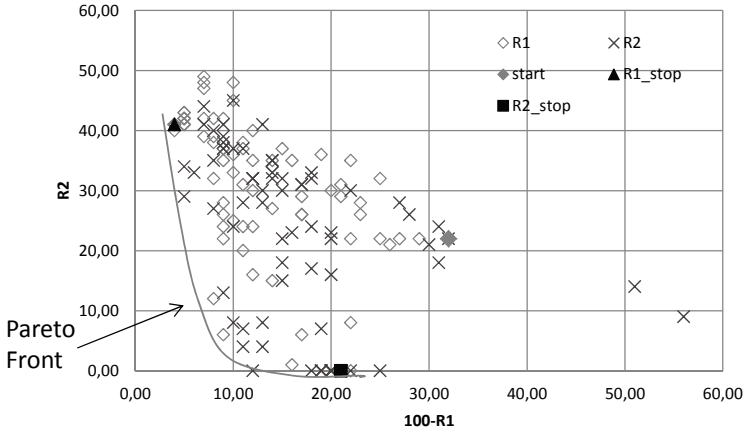

Fig. 2. ESTRA solutions in the objective space. R_1 and R_2 are the solutions found after optimizing R_1 and R_2 functions, respectively; 'start' is the initial solution, whereas R_1_stop and R_2_stop are the solutions

In Table 1 the coordinates of the two optimal points, $P_1(x_1, y_1, z_1)$, $P_2(x_2, y_2, z_2)$, found using ESTRA algorithm are reported, after optimizing separately R_1 and R_2 functions; the same couple of points ('start' in Table 1) was taken as the start. The last two lines report also the value of the R_1 and R_2 functions computed for the two optimal solutions.

Table 1. Optimal injection positions [mm] using ESTRA algorithm. Start: initial points, R_1 and R_2: optimal solutions found considering R_1 and R_2 functions, respectively

		Start	**R_1**	**R_2**
P_1	x_1	−2.0	6.5	−8.3
P_1	y_1	24.0	9.0	−22.3
P_1	z_1	−30.0	−17.8	50.0
P_2	x_2	−16.0	5.5	3.0
P_2	y_2	−6.0	0.6	16.0
P_2	z_2	−30.0	21.5	−41.0
	R_1	68	96	41
	R_2	22	79	0

In turn, using Non dominated Sorting Genetic Algorithm (NSGA) [12, 23] the bi-objective problem is solved and the resulting Pareto front is identified; the relevant results are shown in Figure 3. Filled squares represent the initial generation of twenty individuals (point coordi-

nates and R_1 and R_2 values are reported in Table 2), whereas filled triangles are individuals of the final generation (Table 3) found by means of NSGA after ten generations.

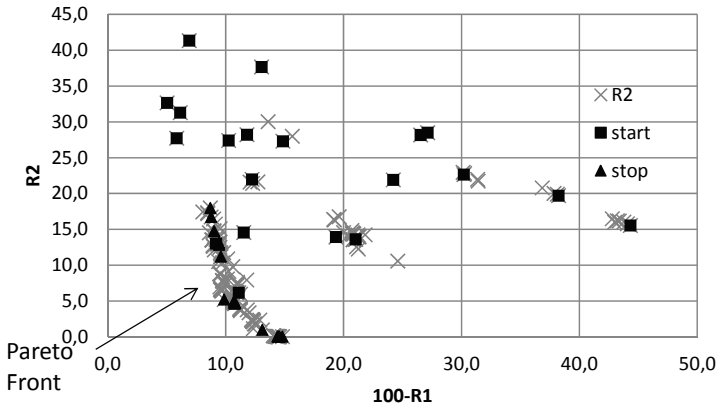

Fig. 3. NSGA solutions in the objective space. R_2 are intermediate solutions found during the optimization; 'start' is the initial set of 20 solutions, whereas 'stop' is the set of 20 final solutions found by means of NSGA algorithm

Table 2. First 20 elements for NSGA algorithms. Point coordinates [mm]

	#1	**#2**	**#3**	**#4**	**#5**	**#6**	**#7**	**#8**	**#9**	**#10**
x_1	40.7	13.9	47.9	39.6	33.9	35.3	34.7	38.3	35.5	5.9
y_1	45.3	27.3	24.3	48.0	37.9	1.6	15.9	39.8	37.7	24.9
z_1	12.7	95.8	80.0	65.6	74.3	27.7	95.0	18.7	27.6	96.0
x_2	45.7	48.2	7.1	1.8	19.6	2.3	1.7	24.5	34.0	17.0
y_2	31.6	7.9	21.1	42.5	32.8	4.9	21.9	22.3	32.8	29.3
z_2	9.8	97.1	91.6	93.4	17.1	82.3	38.2	64.6	16.3	22.4
R_1	55.7	61.8	73.4	75.8	94.1	80.6	87.7	95.0	72.9	90.8
R_2	15.5	19.7	28.2	21.9	27.7	13.9	21.9	32.6	28.5	13.0
	#11	**#12**	**#13**	**#14**	**#15**	**#16**	**#17**	**#18**	**#19**	**#20**
x_1	37.6	27.4	40.7	30.8	45.9	3.8	28.4	15.6	34.5	7.6
y_1	12.8	6.9	12.2	23.7	14.3	2.7	23.5	26.4	37.4	41.3
z_1	50.6	14.9	92.9	35.2	75.7	53.1	1.2	16.6	45.1	53.8
x_2	35.0	12.9	17.5	41.5	37.7	39.0	16.9	30.1	4.2	49.8
y_2	44.5	42.0	9.8	29.3	19.0	46.7	8.1	13.1	11.4	3.9
z_2	95.9	25.4	25.1	55.0	56.8	13.0	79.4	65.4	91.3	44.3
R_1	85.1	69.8	88.4	93.1	87.0	79.0	88.9	93.8	89.7	88.2
R_2	27.3	22.6	14.5	41.3	37.7	13.6	6.1	31.3	27.4	28.2

In Table 3 the coordinates of the twenty optimal points located along the non-dominated front found after ten generations of the NSGA algorithm are reported. In the last two lines the corresponding R_1 and R_2 values are also reported.

Table 3. Optimized points [mm] using NSGA algorithm

	#1	**#2**	**#3**	**#4**	**#5**	**#6**	**#7**	**#8**	**#9**	**#10**
x_1	2.0	1.5	−18.7	−18.4	1.5	2.0	1.7	−19.0	1.5	2.0
y_1	−0.2	−1.6	0.2	0.1	−1.5	−0.3	−1.3	−0.1	−1.6	−0.2
z_1	−49.4	−49.7	47.1	48.2	−49.7	−49.4	−49.0	46.5	−49.7	−49.4
x_2	−7.6	−8.1	−8.7	−8.7	−8.1	−7.5	−8.1	−8.7	−8.1	−7.6
y_2	−15.9	−18.0	1.5	3.6	−17.9	−16.1	−18.3	1.8	−18.0	−16.0
z_2	30.7	36.5	−25.1	−25.6	36.5	30.6	33.8	−22.4	36.7	30.5
R_1	89.3	85.5	91.0	90.6	85.6	89.2	86.9	91.3	85.5	89.3
R_2	4.7	0.0	14.7	13.0	0.0	4.6	0.9	18.0	0.0	4.9
	#11	**#12**	**#13**	**#14**	**#15**	**#16**	**#17**	**#18**	**#19**	**#20**
x_1	2.0	1.5	−18.0	1.3	1.4	−18.3	−19.1	1.8	2.2	−18.3
y_1	−0.2	−1.6	0.2	−0.2	−1.6	0.1	0.2	−1.6	−1.6	−0.1
z_1	−49.4	−49.7	50.0	−50.0	−49.1	47.7	48.0	−50.0	−47.0	47.6
x_2	−7.5	−8.1	−8.7	−7.6	−8.1	−8.7	−8.7	−8.1	−8.1	−8.7
y_2	−15.9	−18.0	1.4	−15.8	−17.2	2.8	1.0	−17.4	−14.2	1.3
z_2	30.7	36.4	−24.2	29.8	38.7	−27.8	−25.6	36.9	33.4	−22.9
R_1	89.2	85.6	90.5	89.3	85.2	90.4	90.5	85.4	90.1	91.2
R_2	4.6	0.0	12.8	5.0	0.0	11.2	13.1	0.0	5.2	16.7

In Figure 4 the colored map of the temperature distribution, corresponding to case #20 in Table 3, is shown for two different orthogonal layers.

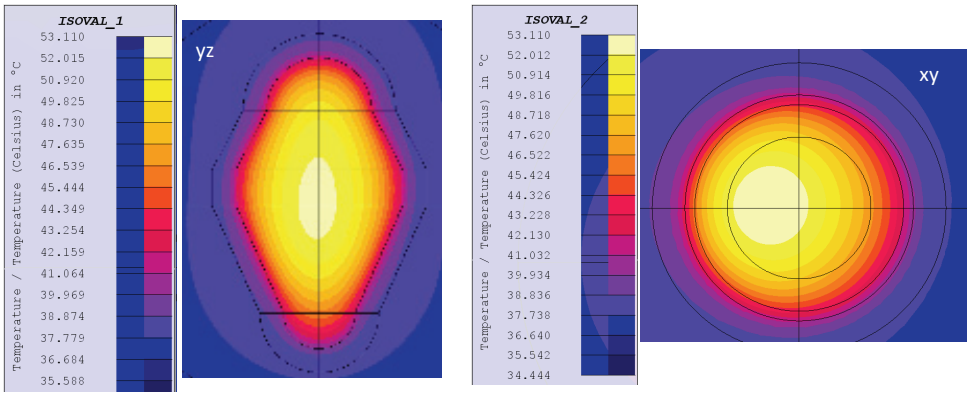

Fig. 4. NSGA solution. Temperature distribution on two orthogonal layers (yz and xy). Case #20 in Table 3

The following remark can be put forward. Lower R_2 values preserve the over-heating of some areas in the tumor region, whereas higher R_1 values ensure the therapeutic temperature in a larger volume of the treated region. Accordingly, solutions that exhibit a higher value of R_1 are better candidates, and this could be a good criterion for extracting a particular solution from the Pareto front. On the other hand, it can be noted that some solutions form a crowded subset of the front (e.g. #3, #4, #16 and #20 or #2, #5, #9 and #12).

5. Conclusions

In the paper a comparative study of results obtained using two optimization techniques have been presented. Actually, the aim of the paper was to synthesize the NPs injections in order to increase the temperature in the tumor up to a therapeutic value. The solutions found put the ground for the systematic approach to the optimal treatment planning in MFH.

References

[1] Goya G.F., Grazú V., Ibarra M.R., *Magnetic Nanoparticles for Cancer Therapy.* Curr. Nanosc. 4: 1-16 (2008).
[2] Rosensweig R.E., *Heating magnetic fluid with alternating magnetic field.* J. Magn. Magn. Mat., pp. 370-374 (2002).
[3] Gneveckow U., Jordan A., Scholz Volker Brüß R. et al., *Description and characterization of the novel hyperthermia and thermoablation-system MFH®300F for clinical magnetic fluid hyperthermia*. Med. Phys. 31(6): 1444-1451 (2004).
[4] Di Barba P., Dughiero F., Sieni E., *Magnetic field synthesis in the design of inductors for magnetic fluid hyperthermia.* IEEE Trans on Magn. 46: 2931-2934 (2010).
[5] Di Barba P., Dughiero F., Trevisan F., *Optimization of the Loney's solenoid through Quasi-analytical strategies,: a benchmark problem reconsidered.* IEEE Trans. Magn. 33: 1864-1867 (1997).
[6] Moroz P., Jones S.K., Gray B.N., *Magnetically mediated hyperthermia: current status and future directions*. Int. J. Hyperthermia 18(4): 267-284 (2002).
[7] Curley S.A., *New Approaches to the Treatment of Hepatic Malignancies. Radiofrequency Ablation of Malignant Liver Tumors.* Annals of Surgical Oncology 10(4): 338-347 (2003).
[8] Candeo A., Dughiero F., *Numerical FEM models for the planning of magnetic induction hyperthermia treatments with nanoparticles*. IEEE Trans. Magn. 45: 1654-1657 (2009).
[9] Salloum M., Ma R., Zhu L., *Enhancements in treatment planning for magnetic nanoparticle hyperthermia: optimization of the heat absorption pattern.* Int. J. of Hyperthermia 25 (2009).
[10] M. Salloum, R. Ma, L. Zhu, *An in-vivo experimental study of temperature elevations in animal tissue during magnetic nanoparticle hyperthermia.* Int. J. Hyperth. 24: 589-601 (2008).
[11] Di Barba P., Dughiero F., Sieni E., Candeo E.A., *Coupled Field Synthesis in Magnetic Fluid Hyperthermia*. Magnetics, IEEE Transactions on 47(5): 914-917 (2010).
[12] Di Barba P., *Multiobjective Shape Design in Electricity and Magnetism*. Springer (2010).
[13] Di Barba P., Palka R., *Optimization of the HTSC-PM Interaction in Magnetic Bearings by a Multiobjective Design.* Proc. Int Symp. Electromagnetic Fields in Mechatronics, Electrical and Electronic Eng. pp. 94-95 (2007).
[14] Di Barba P., Mognaschi M.E., Palka R., Savini A., *Optimization of the MIT Field Exciter by a Multiobjective Design.* IEEE Trans. Magn. 45(3): 1530-1533 (2009).
[15] Binns K.J., Lawrenson P.J., Trowbridge C.W., *The Analytical and Numerical Solution of Electric and Magnetic Fields*. Wiley & Sons Ltd, Chichester (1992).
[16] Carslaw H.S., Jaeger J.C., *Conduction of heat in solids*. Clarendon Press, Oxford (1959).

[17] Pennes H.H., *Analysis of tissue and arterial blood temperatures in the resting human forearm*. J. Appl. Physiol. 85: 5-34 (1948).
[18] Preston T.W., Reece A.B.J., *Solution of 3-Dimensional eddy current problems: the T-Ω method.* IEEE Trans. Magn. 18: 486-491 (1982).
[19] Biro O., Preis K., Vrisk G., Richter K.R., Ticar I., *Computation of 3-D magnetostatic fields using a reduced scalar potential.* IEEE Trans. Magn. 29: 1329-1332 (1993).
[20] www.cedrat.com (last visited January 2012).
[21] Lang J., Erdmann B., Seebass M., *Impact of nonlinear heat transfer on temperature control in regional hyperthermia.* IEEE Trans. Biom. Eng. 46: 1129-1138 (1999).
[22] Di Barba P., Dughiero F., Sieni E., *Synthesizing Distributions of Magnetic Nanoparticles for Clinical Hyperthermia.* IEEE Trans. Magn., in press.
[23] Deb K., Pratap A., Agarwal S., Meyarivan E.T., *A fast and elitist multiobjective genetic algorithm: NSGA-II.* Evolutionary Computation, IEEE Transactions on 6(2): 182-197 (2002).
[24] Hudy W., Jaracz K., *Selection of control parameters in a control system with a DC electric series motor using evolutionary algorithm*. Archives of Electrical Engineering 60(3): 231-237 (2011).